COMMUNICATIONS IN COMPUTATIONAL PHYSICS
Vol. **6**, No. 1, pp. 185-202

Commun. Comput. Phys.
July 2009

A Bilinear Immersed Finite Volume Element Method for the Diffusion Equation with Discontinuous Coefficient†

X.-M. He[1], T. Lin[1,*] and Y. Lin[2,3]

[1] *Department of Mathematics, Virginia Tech, Blacksburg, VA 24060, USA.*
[2] *Department of Mathematical and Statistical Science, University of Alberta, Edmonton AB, T6G 2G1, Canada.*
[3] *Department of Applied Mathematics, The Hong Kong Polytechnic University, Kowloon, Hong Kong.*

Received 17 December 2007; Accepted (in revised version) 6 June 2008

Available online 24 November 2008

Abstract. This paper is to present a finite volume element (FVE) method based on the bilinear immersed finite element (IFE) for solving the boundary value problems of the diffusion equation with a discontinuous coefficient (interface problem). This method possesses the usual FVE method's local conservation property and can use a structured mesh or even the Cartesian mesh to solve a boundary value problem whose coefficient has discontinuity along piecewise smooth nontrivial curves. Numerical examples are provided to demonstrate features of this method. In particular, this method can produce a numerical solution to an interface problem with the usual $\mathcal{O}(h^2)$ (in L^2 norm) and $\mathcal{O}(h)$ (in H^1 norm) convergence rates.

AMS subject classifications: 65N15, 65N30, 65N50, 35R05

Key words: Interface problems, immersed interface, finite volume element, discontinuous coefficient, diffusion equation.

1 Introduction

In many applications, a simulation domain is often formed by several materials separated by curves or surfaces from each other, and this often leads to the so called interface problem consisting of the usual boundary value problem of the diffusion equation, the usual boundary condition, plus jump conditions across the material interface

†This paper is dedicated to Richard E. Ewing on the occasion of his 60th birthday.

*Corresponding author. *Email addresses:* `xiaoming@vt.edu` (X.-M. He), `tlin@vt.edu` (T. Lin), `yanlin@ualberta.ca` (Y. Lin)

required by pertinent physics. It is well known that efficiently solving this type of interface problem is critical in many applications of engineering and sciences, including flow problems [10, 11, 27, 29, 30, 43, 52], electromagnetic problems [4, 16, 61, 66–70, 78], shape/topology optimization problems [13–15, 29, 36–38, 46, 74], and the modeling of nonlinear phenomena [41, 79, 86], to name just a few. In this paper, we present a finite volume element method with bilinear immersed finite element (IFE) [39, 59] for solving this popular interface problem. This method possesses both the advantages of finite volume element method and those of IFE. In particular, this method can use a Cartesian mesh to solve a boundary value problem with a discontinuous coefficient whose interface consists of nontrivial piecewise smooth curves.

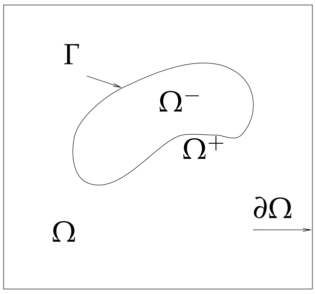

Figure 1: A sketch of the domain for the interface problem.

To be specific, we consider the following boundary value problem:

$$-\nabla\cdot(\beta\nabla u)=f, \quad (x,y)\in\Omega, \tag{1.1}$$

$$u|_{\partial\Omega}=g. \tag{1.2}$$

Here, see the sketch in Fig. 1, without loss of generality, we assume that $\Omega\subset IR^2$ is a rectangular domain, the interface Γ is a curve separating Ω into two sub-domains Ω^-, Ω^+ such that $\overline{\Omega}=\overline{\Omega^-}\cup\overline{\Omega^+}\cup\Gamma$, and the coefficient $\beta(x,y)$ is a piecewise constant function defined by

$$\beta(x,y)=\begin{cases}\beta^-, & (x,y)\in\Omega^-,\\ \beta^+, & (x,y)\in\Omega^+.\end{cases}$$

Because of the discontinuity in the coefficient β, jump conditions are also imposed on the interface Γ:

$$[u]|_\Gamma=0, \tag{1.3}$$

$$\left[\beta\frac{\partial u}{\partial n}\right]|_\Gamma=0. \tag{1.4}$$

Of course, conventional numerical methods can be used to solve interface problem (1.1)-(1.4). Standard discretization techniques such as finite difference (FD), see [73] and references therein, finite volume (FV), see [40] and references therein, and finite element

(FE), see [5, 17, 25] and references therein, are all applicable, provided that meshes used by these methods are tailored to resolve the interfaces, see Fig. 2. Otherwise, the lack of smoothness in the exact solution across the interface will prevent a numerical method to perform satisfactorily [9, 17, 25]. In general, this requires a conventional method to use a mesh such that each of its element is basically occupied by one of the materials, and consequently, this prevents the usage of a structured mesh such as a Cartesian mesh if the interface is nontrivial. Therefore, conventional methods have limitations for them to solve interface problems efficiently in many applications. As an incomplete list of their limitations, we first note that for applications with moving interfaces, the meshes used by these methods have to be regenerated again and again according to current location of the interfaces at the moment the interface problems have to be solved. Second, there are many applications in which structured meshes are preferred, for example, Particle In Cell method for Plasma Particle Simulation, see [48, 62] and references therein. Last, but not the least, we note that the algebraic system based on a structured mesh often requires much less computational time to solve because efficient algebraic solvers such as fast FFT and multigrid can be easily implemented.

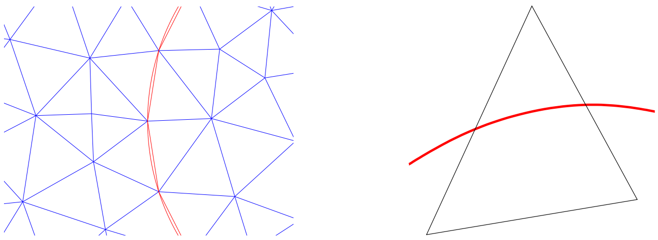

Figure 2: The plot on the left shows how elements are placed along an interface in a standard FE method. Each of the elements is essentially on one side of the interface. An element not allowed in a standard FE method is illustrated by the plot on the right.

To alleviate these limitations, FD methods are modified by reformulating the interface problem in elements cut through by interface or by employing finite difference stencils sophisticated enough to capture the discontinuity at the nodes in the neighborhood of the interface. Along this direction, Peskin's immersed boundary method [71,72] is one of the early representative ideas followed by many publications with applications in numerous fields [3,21,26,28,31,35,42,45,49–51,53,55,65,80,81,84,85]. For FE methods, special local basis functions have been developed to handle the interface jump conditions in elements cut through by interface. Early work can be found in [8] and [6,7], which have developed basis functions for treating rough coefficients. Further development can be found in the partition of unity methods and the extended finite element methods (X-FEMs) [12,64,77]. Another class of FE methods along this idea are the recently introduced immersed finite element (IFE) methods [1, 2, 22, 33, 39, 47, 48, 54, 57–60, 76]. More references can also be found in [56].

We like to point out that the early works by Babuska et al. in [5–7] proposed and analyzed several classes of finite element methods for interface problems, in particular for linear element in one-dimension, these are equivalent or identical to the linear immersed finite elements, therefore the work [54] is just a special case of [5–7] with somewhat different settings. However for high order elements in one-dimension the immersed finite element proposed in [1, 2, 59, 60] and etc are different from those in [5–7].

In IFE methods, standard finite element functions are used in elements occupied by one of the materials, but piecewise polynomials patched by interface jump conditions are employed in elements formed by multiple materials. Particularly, the meshes used by IFE methods can be independent of the interface; hence, structured meshes, even the Cartesian mesh, can be used to solve boundary value problems with rather sophisticated interfaces between materials.

Up to now, IFE has been applied to solve interface problems in the Galerkin formulation, see [1, 2, 22, 47, 54, 57–60]. On the other hand, finite volume element (FVE) has the local conservation property which is very much desired in many applications, see [18–20,23,24,32,34,44,63,75,82] and related reference therein. We believe that the combination of the FVE's local conservation property and IFE's flexibility to handle interface jump conditions without using complicated meshes can generate competitive numerical methods for solving interface problems.

The rest of this article is organized as follows. In Section 2, we recall the definition of the bilinear IFE space to be used and its basic features. In Section 3, we present the finite volume element method based on this bilinear IFE space. In Section 4, we present several numerical examples to demonstrate features of this immersed FVE method. The conclusion is given in Section 5.

2 The bilinear immersed finite element space

In this section, we recall the bilinear IFE space discussed in [39,59]. We will also list some of its basic properties and refer reader to the references above for more details.

Let $\mathcal{T}_h$, $h>0$ be a family of rectangular meshes of the solution domain Ω that can be a union of rectangles. For each mesh $\mathcal{T}_h$, we let

$$\mathcal{N}_h=\{X_i,\ i=1,2,\cdots,N\}$$

be the set of its nodes, and let $\mathcal{N}_h^\circ=\mathcal{N}_h\cap\Omega$. We first consider a typical rectangle element $T\in\mathcal{T}_h$ assuming that the vertices of T are A_i, $i=1,2,3,4$, with $A_i=(x_i,y_i)^t$. For a nontrivial interface Γ, some of the elements in a mesh will be cut through by Γ and we will call them interface elements. The meaning of non-interface elements is obvious. If T is an interface element, then we use $D=(x_D,y_D)^T$ and $E=(x_E,y_E)^T$ to denote the intersection points of Γ and the edge of T. In general, there are two types of rectangular interface elements. Type I are those for which the interface intersects two of its adjacent edges; Type II are those for which the interface intersects two of its opposite edges, see Fig. 3.

The basic idea of IFE method is to use standard finite element functions in non-interface elements, and use special finite element functions in interface elements that are

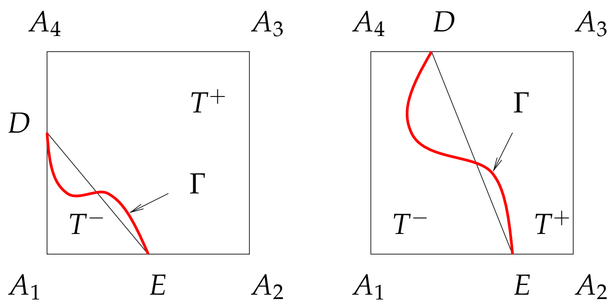

Figure 3: Two typical interface elements. The element on the left is of Type I while the one on the right is of Type II.

constructed according to jump conditions across the interface. Hence, our main concern is the finite element functions in a typical interface element $T \in \mathcal{T}_h$. Note that the interface Γ separates an interface element T into two subsets $T^s = T \cap \Omega^s$, $s = \pm$. This suggests us to form a piecewise function with two bilinear polynomials on T patched up together by interface jump conditions as follows:

$$\phi(x,y) = \begin{cases} \phi^-(X) = \phi^-(x,y) = a^- x + b^- y + c^- + d^- xy, & X = (x,y) \in T^-, \\ \phi^+(X) = \phi^+(x,y) = a^+ x + b^+ y + c^+ + d^+ xy, & X = (x,y) \in T^+, \\ \phi^-(D) = \phi^+(D), \ \phi^-(E) = \phi^+(E), \ \phi^-(\frac{D+E}{2}) = \phi^+(\frac{D+E}{2}), \\ \int_{\overline{DE}} \left(\beta^- \frac{\partial \phi^-}{\partial \mathbf{n}_{\overline{DE}}} - \beta^+ \frac{\partial \phi^+}{\partial \mathbf{n}_{\overline{DE}}} \right) ds = 0, \end{cases} \tag{2.1}$$

where $\mathbf{n}_{\overline{DE}}$ is the unit vector perpendicular to the line $\overline{DE}$. Further, we let $\phi_i(X)$ be the piecewise linear function described by (2.1) such that

$$\phi_i(A_j) = \phi_i(x_j,y_j) = \begin{cases} 1, & \text{if } i = j, \\ 0, & \text{if } i \neq j \end{cases} \tag{2.2}$$

for $1 \le i,\ j \le 4$. We then introduce the local bilinear IFE space on element $T \in \mathcal{T}_h$:

$$S_h(T) = span\{\phi_i, i = 1,2,3,4\},$$

where ϕ_i, $i = 1,2,3,4$ are the usual bilinear nodal basis functions if T is a non-interface element; otherwise, ϕ_i, $i = 1,2,3,4$ are the piecewise bilinear polynomials defined by (2.1) and (2.2). Then, for each node $X_i \in \mathcal{N}_h$, we define $\Phi_i(X) = \Phi_i(x,y)$ to be a piecewise bilinear function such that $\Phi_i|_T \in S_h(T)$, $\Phi_i(X_j) = \delta_{ij}$, $\forall T \in \mathcal{T}_h$. Finally, we define the bilinear IFE space on Ω by $S_h(\Omega) = span\{\Phi_i(X) \mid X_i \in \mathcal{N}_h\}$.

The word "immersed" is used for this finite element space just to emphasize the fact that the mesh can be independent of the interface such that the interface can be immersed inside elements of this mesh. Fig. 4 illustrates the difference between the bilinear IFE local nodal basis function and the standard bilinear local nodal basis functions. Fig. 5 provides a sketch of the surface of a global bilinear IFE basis function over its support.

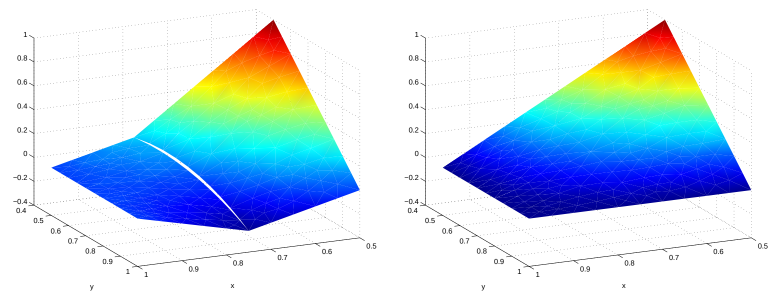

Figure 4: The plot on the left is for one of the bilinear IFE local nodal basis functions, the plot on the right is the corresponding regular bilinear local nodal basis function on the same element.

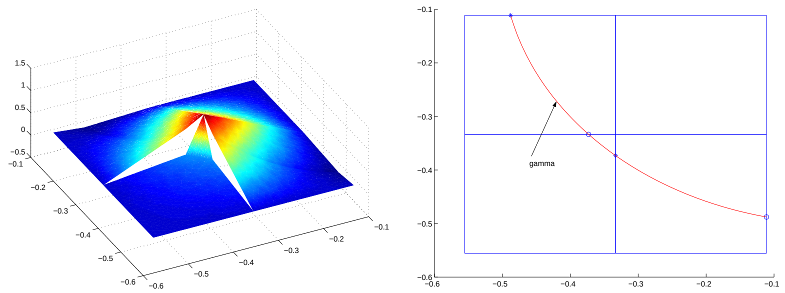

Figure 5: The plot on the left is the surface of one global bilinear IFE basis over its support, the plot on the right shows the elements forming the support and the interface

We now list some basic properties of $S_h(\Omega)$, and we refer readers to [39] for details. From now on, for a given function $f(X)$, we let $f^s = f|_{\Omega^s}$, $s = \pm$.

• For a given rectangular mesh, the IFE space $S_h(\Omega)$ has the same number of nodal basis functions as that in the usual bilinear FE space.

• For a rectangular mesh $\mathcal{T}_h$ fine enough, most of its elements are non-interface elements, and most of the nodal basis functions of the IFE space $S_h(\Omega)$ are just the usual bilinear nodal basis functions except for few nodes in the vicinity of the interface Γ.

• For any $\phi \in S_h(\Omega)$, we have

$$\phi|_{\Omega\backslash\Omega'} \in H^1(\Omega\backslash\Omega'),$$

where Ω' is the union of interface rectangles.

• If $\Gamma \cap T$ is a line segment, then

$$\phi^-|_{\Gamma\cap T} = \phi^+|_{\Gamma\cap T}, \quad \forall \phi \in S_h(\Omega).$$

• Every function $\phi \in S_h(T)$ satisfies the flux jump condition on $\Gamma \cap T$ exactly in a weak sense as follows:

$$\int_{\Gamma\cap T} (\beta^- \nabla\phi^- - \beta^+ \nabla\phi^+) \cdot \mathbf{n}_{\Gamma} ds = 0.$$

• The bilinear IFE local nodal basis functions on an interface element T satisfy the partition of unity, i.e.,

$$\phi_1(X)+\phi_2(X)+\phi_3(X)+\phi_4(X)=1, \quad \forall X\in T.$$

• The bilinear IFE space is consistent with the usual bilinear finite element space in the sense that when $\beta^-=\beta^+$, we have

$$\phi^-=\phi^+$$

and ϕ become a usual bilinear polynomial for any $\phi\in S_h(T)$, $\forall\, T\in\mathcal{T}_h$.

• The bilinear IFE space $S_h(\Omega)$ has the usual approximation capability expected:

$$\|I_hu-u\|_{0,T}+h\|I_hu-u\|_{1,T}\leq Ch^2$$

provided that u has the required regularity.

Remark 2.1. It is possible to extend the method in this article to handle variable discontinuous coefficient and non-homogeneous jump conditions. In order to deal with the variable discontinuous coefficients, we need to replace the constants β^- and β^+ in (2.1) by the corresponding variable discontinuous coefficients. The idea of homogenization by using level-set method from [83] seems to be a viable approach to treat non-homogeneous jump conditions.

3 The immersed finite volume element method

Since the bilinear IFE space has the usual approximation capability expected from bilinear polynomials [39], we now apply it to solve the interface problem of the diffusion equation in the finite volume element formulation. To describe the method, for each mesh $\mathcal{T}_h$ of Ω, we introduce a dual mesh $\widehat{\mathcal{T}}_h$ by connecting the nearby centers of the elements in $\mathcal{T}_h$ in the vertical and horizontal directions, see the illustration in Fig. 6 where the dual mesh $\widehat{\mathcal{T}}_h$ is sketched by the dash lines while $\mathcal{T}_h$ is sketched by solid lines.

First, we derive a weak form on each element of the dual mesh. Assume that the source term $f(X)$ is smooth enough so that the exact solution has the required smoothness in the discussion below. Let $\widehat{K}_i$ be an element of $\widehat{\mathcal{T}}_h$ containing the node X_i of $\mathcal{T}_h$. First, we integrate the differential equation (1.1) over $\widehat{K}_i$ to have

$$-\int_{\widehat{K}_i}\nabla\cdot(\beta\nabla u)\,dxdy=\int_{\widehat{K}_i}f\,dxdy. \tag{3.1}$$

If $\widehat{K}_i$ is not an interface element, then a straightforward application of the Green's formula leads to

$$-\int_{\partial\widehat{K}_i}\beta\frac{\partial u}{\partial\mathbf{n}}\,ds=\int_{\widehat{K}_i}f\,dxdy. \tag{3.2}$$

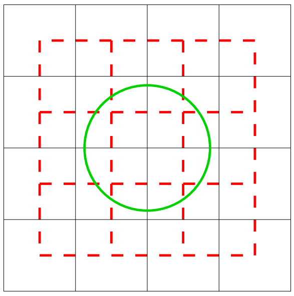

Figure 6: A mesh of Ω and the dual mesh for an interface problem. Elements in the mesh are solid rectangles and elements in the dual mesh are dash rectangles.

If $\widehat{K}_i$ is an interface element, then, by applying the Green's formula piecewisely, we have

$$\begin{aligned} -\int_{\widehat{K}_i^-} \nabla\cdot(\beta\nabla u)\, dxdy - \int_{\widehat{K}_i^+} \nabla\cdot(\beta\nabla u)\, dxdy &= \int_{\widehat{K}_i} f\, dxdy, \\ -\int_{\partial\widehat{K}_i^-} \beta\frac{\partial u}{\partial \mathbf{n}}\, ds - \int_{\partial\widehat{K}_i^+} \beta\frac{\partial u}{\partial \mathbf{n}}\, ds &= \int_{\widehat{K}_i} f\, dxdy, \\ -\int_{\partial\widehat{K}_i} \beta\frac{\partial u}{\partial \mathbf{n}}\, ds - \int_{\partial\widehat{K}\cap\Gamma} \left[\beta\frac{\partial u}{\partial \mathbf{n}}\right]_\Gamma ds &= \int_{\widehat{K}_i} f\, dxdy, \end{aligned}$$

which leads to (3.2) again because of the flux jump condition (1.4). Hence, we conclude that the weak form (3.2) holds for any element $\widehat{K}_i \in \widehat{\mathcal{T}}_h$. This weak form enables us to introduce the bilinear immersed FVE method as follows: find $u_h \in S_{h,E}(\Omega)$ such that

$$-\int_{\partial\widehat{K}_i} \beta\frac{\partial u_h}{\partial \mathbf{n}}\, ds = \int_{\widehat{K}_i} f\, dxdy, \quad \forall X_i \in \mathcal{N}_h^\circ. \tag{3.3}$$

Here, $S_{h,E}(\Omega) = \{v_h \in S_h(\Omega), v_h(X) = g(X)\ \forall X \in \mathcal{N}_h \cap \partial\Omega\}$. We would like to point out that (3.3) indicates that the immersed FVE solution also have the local conservation property.

We now discuss some details in the implementation of the bilinear immersed FVE method. The key issue is the integrals used in this method. On each non-interface element $\widehat{K}_i$, standard Gaussian quadratures can be applied because we can assume that all the integrands involved are smooth enough. If $\widehat{K}_i$ is an interface element, both the line integral and the area integral in the bilinear immersed FVE method need to be treated carefully because of the discontinuity across the interface.

First, let us consider the area integral $\int_{\widehat{K}_i} f\, dxdy$ on the right hand side of (3.3). Under the assumption that $f(X)$ is piecewise smooth with respect to the interface Γ, we can approximate its integration over $\widehat{K}_i$ piecewisely by suitably partitioning $\widehat{K}_i$ into several sub-triangles. Assume that $\widehat{K}_i$ has vertices $\hat{X}_j$, $j = 1,2,3,4$ and interface Γ intersects with the boundary of $\widehat{K}_i$ at D and E on two adjacent edges, see Fig. 7. We can then use points D and E to partition $\widehat{K}_i$ into 4 triangles by adding 3 line segments: $\overline{DE}$, $\overline{D\hat{X}_3}$, $\overline{E\hat{X}_3}$. Note that the last two line segments are formed by connecting D and E to the vertex of $\widehat{K}_i$ not on the edges containing D and E. Hence,

$$\int_{\widehat{K}_i} f\,dxdy = \int_{\triangle_{\hat{X}_1 ED}} f^-\,dxdy + \int_{\triangle_{E\hat{X}_2\hat{X}_3}} f^+\,dxdy + \int_{\triangle_{D\hat{X}_3\hat{X}_4}} f^+\,dxdy + \int_{\triangle_{DE\hat{X}_3}} f^+\,dxdy.$$

Gaussian quadratures with enough degree of precision can be applied straightforwardly to handel integrations on those sub-triangles within either Ω^- or Ω^+. A little extra care is need to handle the sub-triangles whose interiors intersect both Ω^- and Ω^+. For the case illustrated in Fig. 7, when applying a Gaussian quadrature to compute $\int_{\triangle_{DE\hat{X}_3}} f^+\,dxdy$, we can replace the value of f at a quadrature node outside Ω^+ by the value of f at a point on Γ so long as this replacement has an $\mathcal{O}(h^2)$ accuracy which can be achieved if Γ is smooth enough within $\widehat{K}_i$ [25]. A similar procedure can be developed for handling the case in which the interface Γ intersect with the boundary of $\widehat{K}_i$ at D and E on two opposite edges.

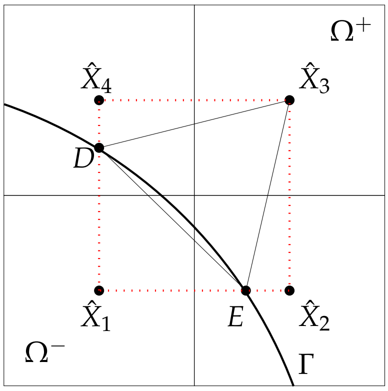

Figure 7: A dual element $\widehat{K} = \square \hat{X}_1\hat{X}_2\hat{X}_3\hat{X}_4 \in \widehat{\mathcal{T}}_h$ sketched by dash lines and 4 adjacent elements of $\mathcal{T}_h$. This element can be partitioned into 4 sub-triangles for the area integrals in the immerse FVE method.

For an interface element $\widehat{K}_i$, the line integral on the left hand side of (3.3) also needs to be treated piecewisely to handle the discontinuity. Again, let us consider a dual element $\widehat{K}_i = \square \hat{X}_1\hat{X}_2\hat{X}_3\hat{X}_4$, see Fig. 8. Since $\widehat{K}_i$ has 4 edges, we have

$$-\int_{\partial \widehat{K}_i} \beta \frac{\partial u_h}{\partial \mathbf{n}}\,ds = -\int_{\overline{\hat{X}_1\hat{X}_2}} \beta \frac{\partial u_h}{\partial \mathbf{n}}\,ds - \int_{\overline{\hat{X}_2\hat{X}_3}} \beta \frac{\partial u_h}{\partial \mathbf{n}}\,ds - \int_{\overline{\hat{X}_3\hat{X}_4}} \beta \frac{\partial u_h}{\partial \mathbf{n}}\,ds - \int_{\overline{\hat{X}_4\hat{X}_1}} \beta \frac{\partial u_h}{\partial \mathbf{n}}\,ds$$

Note that the flux $\beta\frac{\partial u_h}{\partial \mathbf{n}}$ on the boundary of $\widehat{K}_i$ is discontinuous at the points where $\partial\widehat{K}_i$ intersects either the edges of $\mathcal{T}_h$ or the interface Γ. Therefore, the line integrals on the

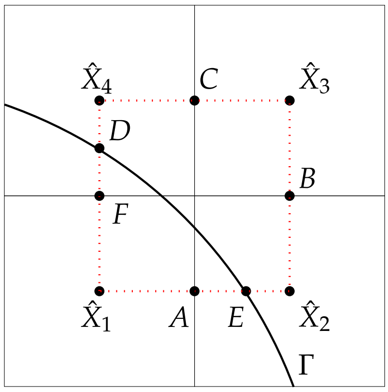

Figure 8: A dual element $\widehat{K}_i = \square \hat{X}_1\hat{X}_2\hat{X}_3\hat{X}_4 \in \widehat{\mathcal{T}}_h$ sketched by dash lines and 4 adjacent elements of $\mathcal{T}_h$. The edges of $\widehat{K}_i$ is partitioned by the discontinuous points of the flux for the line integrals in the immersed FVE method.

right hand side above need to be computed on the small line segments between these discontinuous points. For the example demonstrated in Fig. 8, we have

$$\begin{aligned}
&\int_{\overline{\hat{X}_1\hat{X}_2}} \beta \frac{\partial u_h}{\partial \mathbf{n}}\, ds = \int_{\overline{\hat{X}_1 A}} \beta^- \frac{\partial u_h}{\partial \mathbf{n}}\, ds + \int_{\overline{AE}} \beta^- \frac{\partial u_h}{\partial \mathbf{n}}\, ds + \int_{\overline{E\hat{X}2}} \beta^+ \frac{\partial u_h}{\partial \mathbf{n}}\, ds,\\
&\int_{\overline{\hat{X}_2\hat{X}_3}} \beta \frac{\partial u_h}{\partial \mathbf{n}}\, ds = \int_{\overline{\hat{X}_2 B}} \beta^+ \frac{\partial u_h}{\partial \mathbf{n}}\, ds + \int_{\overline{B\hat{X}_3}} \beta^+ \frac{\partial u_h}{\partial \mathbf{n}}\, ds,\\
&\int_{\overline{\hat{X}_3\hat{X}_4}} \beta \frac{\partial u_h}{\partial \mathbf{n}}\, ds = \int_{\overline{\hat{X}_3 C}} \beta^+ \frac{\partial u_h}{\partial \mathbf{n}}\, ds + \int_{\overline{C\hat{X}_4}} \beta^+ \frac{\partial u_h}{\partial \mathbf{n}}\, ds,\\
&\int_{\overline{\hat{X}_4\hat{X}_1}} \beta \frac{\partial u_h}{\partial \mathbf{n}}\, ds = \int_{\overline{\hat{X}_4 D}} \beta^+ \frac{\partial u_h}{\partial \mathbf{n}}\, ds + \int_{\overline{DF}} \beta^- \frac{\partial u_h}{\partial \mathbf{n}}\, ds + \int_{\overline{F\hat{X}_1}} \beta^- \frac{\partial u_h}{\partial \mathbf{n}}\, ds.
\end{aligned}$$

We note that all the integrands in the line integrals on the right hand sides above are polynomials; hence, a Gaussian quadrature with enough degree precision can be used to compute all of them precisely. As a consequence, this leads to another interesting fact that the matrix in the immersed FVE can be assembled exactly even if the interface Γ is a general curve. On the contrary, the matrices in the immersed finite element methods [39, 48, 57–59] cannot be formed precisely unless the interface Γ is trivial. In assembling the matrix in any of these immersed finite element methods over an interface element $K \in \mathcal{T}_h$, assuming that the interface Γ intersects the edges of K at D and E, the error in the computation of the area integral over the region enclosed by $\overline{DE}$ and Γ is inevitable if Γ is a general curve.

Finally, we would like to point out that, for any given rectangular mesh $\mathcal{T}_h$ of Ω, the algebraic system of this bilinear immersed FVE method has the same structure as the algebraic system in the usual bilinear finite element method for the Dirichlet boundary value problem of the Poisson equation. The matrix in its algebraic system is guaranteed to be symmetric positive definite.

Table 1: Errors of the FV-IFE solution for the case with $\beta^-=1$, $\beta^+=10$.

h	$\|u_h-u\|_0$	$\|u_h-u\|_1$	$\|u_h-u\|_\infty$
1/8	7.7394×10^{-3}	1.1705×10^{-1}	2.5110×10^{-3}
1/16	1.9658×10^{-3}	5.8644×10^{-2}	6.5026×10^{-4}
1/32	4.8127×10^{-4}	2.9255×10^{-2}	1.6598×10^{-4}
1/64	1.2173×10^{-4}	1.4550×10^{-2}	4.1413×10^{-5}
1/128	3.0115×10^{-5}	7.2699×10^{-3}	1.0611×10^{-5}
1/256	7.5436×10^{-6}	3.6362×10^{-3}	2.6485×10^{-6}

Table 2: Errors of the FV-IFE solution for the case with $\beta^-=1$, $\beta^+=10000$.

h	$\|u_h-u\|_0$	$\|u_h-u\|_1$	$\|u_h-u\|_\infty$
1/8	1.8420×10^{-3}	4.1025×10^{-2}	1.4562×10^{-3}
1/16	4.0555×10^{-4}	2.1051×10^{-2}	4.2813×10^{-4}
1/32	7.6016×10^{-5}	1.0193×10^{-2}	2.5606×10^{-4}
1/64	2.4890×10^{-5}	4.8512×10^{-3}	5.0649×10^{-5}
1/128	5.1332×10^{-6}	2.4100×10^{-3}	1.8048×10^{-5}
1/256	1.1050×10^{-6}	1.2110×10^{-3}	4.7363×10^{-6}

4 Numerical examples

In this section, we present numerical examples for the bilinear immersed finite volume element method to illustrate its features. We consider the interface problem defined by (1.1)-(1.4) on the typical rectangular domain $\Omega=[-1,1]\times[-1,1]$. The interface curve Γ is a circle with radius $r_0=\pi/6.28$ that separates Ω into two sub-domains Ω^- and Ω^+ with $\Omega^-=\{(x,y)\mid x^2+y^2\le r_0^2\}$. The coefficient function is

$$\beta(x,y)=\begin{cases}\beta^-, & (x,y)\in\Omega^-,\\ \beta^+, & (x,y)\in\Omega^+.\end{cases}$$

The boundary condition function $g(x,y)$ and the source term $f(x,y)$ are chosen such that the following function u is the exact solution.

$$u(x,y)=\begin{cases}\dfrac{r^\alpha}{\beta^-}, & \text{if } r\le r_0,\\ \dfrac{r^\alpha}{\beta^+}+\left(\dfrac{1}{\beta^-}-\dfrac{1}{\beta^+}\right)r_0^\alpha, & \text{otherwise,}\end{cases} \tag{4.1}$$

with $\alpha=5$, $r=\sqrt{x^2+y^2}$. For simplicity, we only use the simple rectangular Cartesian meshes in our numerical experiments.

Table 1 contains the errors of the bilinear immersed FVE solution u_h with various mesh size h and $\beta^-=1$, $\beta^+=10$. Table 2 contains the errors of the bilinear immersed FVE solution u_h with $\beta^-=1$, $\beta^+=10000$ representing a large jump. Table 3 contains the errors

Table 3: Errors of the FV-IFE solution for the case with $\beta^- = 10$, $\beta^+ = 1$.

h	$\\|u_h-u\\|_0$	$\|u_h-u\|_1$	$\\|u_h-u\\|_\infty$
1/8	7.6119×10^{-2}	1.0927×10^{0}	2.6593×10^{-2}
1/16	1.9110×10^{-2}	5.4809×10^{-1}	6.6274×10^{-3}
1/32	4.7894×10^{-3}	2.7425×10^{-1}	1.6796×10^{-3}
1/64	1.1967×10^{-3}	1.3715×10^{-1}	4.1590×10^{-4}
1/128	2.9946×10^{-4}	6.8576×10^{-2}	1.0489×10^{-4}
1/256	7.4846×10^{-5}	3.4288×10^{-2}	2.6144×10^{-5}

Table 4: Errors of the FV-IFE solution for the case with $\beta^- = 10000$, $\beta^+ = 1$.

h	$\\|u_h-u\\|_0$	$\|u_h-u\|_1$	$\\|u_h-u\\|_\infty$
1/8	7.6026×10^{-2}	1.0927×10^{0}	2.6270×10^{-2}
1/16	1.9119×10^{-2}	5.4813×10^{-1}	6.7172×10^{-3}
1/32	4.7613×10^{-3}	2.7425×10^{-1}	1.6608×10^{-3}
1/64	1.1930×10^{-3}	1.3714×10^{-1}	4.0496×10^{-4}
1/128	2.9813×10^{-4}	6.8575×10^{-2}	1.0940×10^{-4}
1/256	7.4494×10^{-5}	3.4288×10^{-2}	2.6902×10^{-5}

of the bilinear immersed FVE solution u_h with various mesh size h and $\beta^- = 10$, $\beta^+ = 1$. Table 4 contains the errors of the bilinear immersed FVE solution u_h with $\beta^- = 10000$, $\beta^+ = 1$. In these tables, $\|\cdot\|_0$ represents the usual L^2 norm, $|\cdot|_1$ is the usual semi-H^1 norm, and of course, they are computed numerically according to the mesh used. The quantity $\|\cdot\|_\infty$ is the discrete infinity norm which is the maximum of the absolute values of the given function at all the nodes of a mesh.

We can easily see that the data in the second and third columns of these tables satisfy

$$\|u_h-u\|_0 \approx \frac{1}{4}\|u_{\hat{h}}-u\|_0, \quad |u_h-u|_1 \approx \frac{1}{2}|u_{\hat{h}}-u|_1,$$

for $h=\hat{h}/2$. Using linear regression, we can see that the data in Table 1 obey

$$\|u_h-u\|_0 \approx 0.5008h^{2.0024}, \quad |u_h-u|_1 \approx 0.9427\, h^{1.0025}, \quad \|u_h-u\|_\infty \approx 0.1559\, h^{1.9788};$$

the data in Table 2 obey

$$\|u_h-u\|_0 \approx 0.1422\, h^{2.1154}, \quad |u_h-u|_1 \approx 0.3514\, h^{1.0246}, \quad \|u_h-u\|_\infty \approx 0.0486\, h^{1.6390};$$

the data in Table 3 obey

$$\|u_h-u\|_0 \approx 4.8643\, h^{1.9983}, \quad |u_h-u|_1 \approx 8.7375\, h^{0.9990}, \quad \|u_h-u\|_\infty \approx 1.6923\, h^{1.9974};$$

and the data in Table 4 obey

$$\|u_h-u\|_0 \approx 4.8715\, h^{1.9995}, \quad |u_h-u|_1 \approx 8.7379\, h^{0.9990}, \quad \|u_h-u\|_\infty \approx 1.6301\, h^{1.9861}.$$

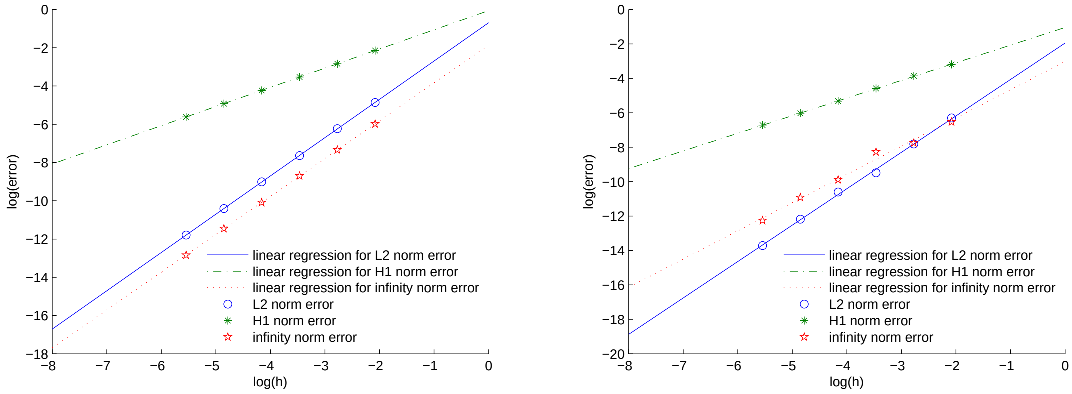

Figure 9: The plot on the left is for the linear regression of the data in Table 1 and the plot on the right is for the linear regression of the data in Table 2.

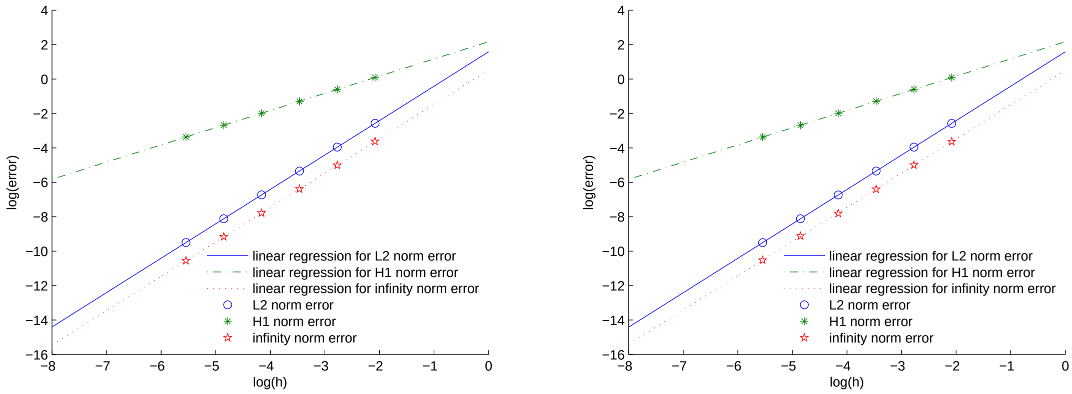

Figure 10: The plot on the left is for the linear regression of the data in Table 3 and the plot on the right is for the linear regression of the data in Table 4.

See Figs. 9 and 10 for these linear regressions. These results further indicates that the bilinear immersed IVE solution u_h converges to the exact solution with convergence rates $\mathcal{O}(h^2)$ and $\mathcal{O}(h)$ in the L^2 norm and H^1 norm, respectively. However, the actual computational results show that the solution does not always have the second order convergence in the L^∞ norm even though the mesh is fine enough. Similar phenomenon has been observed for IFE method, see [39,57]. We guess this is mainly due to the non-conforming feature of the IFE space, and we plan to investigate this issue in our future research.

For a given rectangular mesh of Ω, we note that the linear system in this bilinear immerse IVE method has the same structure as that in the IVE method based on the standard bilinear finite elements for the Poisson's equation, especially from the point view of the number of non-zero entries and their locations in the matrix of the related linear system. This suggests that, on any given computer, the CPU time needed to solve the

Table 5: Comparison of the computational costs for solving linear systems in both the bilinear FVE method and the bilinear immersed FVE method.

	bilinear FVE	$\beta^+:\beta^-=1:1.1$	$\beta^+:\beta^-=1:2$	$\beta^+:\beta^-=1:10$
# of iterations	221	222	279	299

bilinear immerse FVE method should be comparable to that needed to solve the linear system in the standard bilinear FVE for simple Poisson's equation. Since it has become more and more difficult to obtain the precise CPU time usage of a computational procedure on a modern computer because of the complexity of the CUP unit (multi cores, cache, hardware parallelization, etc.) and the software (operating system, fire-wall, virus scan, etc.), we choose the number of iterations needed to make the preconditioned conjugate gradient (PCG) method to converge for a given error tolerance to illustrate the above observation, see Table 5. For the Ω specified at the beginning of this section, we use a rectangular mesh with $h=1/128$, the incomplete Cholesky preconditioner, and the error tolerance $tol=10^{-10}$ in all the computations. From this table, we can see that, while the linear system in the bilinear FVE method for the Poisson's equations uses 221 PCG iterations, the linear system in the bilinear immersed FVE method uses a 222 PCG iteration for the interface problem described in this section with $\beta^+:\beta^-=1:1.1$. We have also observed that the number of PCG iterations needed by the bilinear immersed FVE method gradually increases as the ratio $\beta^+:\beta^-$ becomes larger. This increase is due to the fact that the interface problem is essentially more difficult than the simple boundary value problem of the Poisson's equation and will inevitably cost more time to solve by any method.

5 Conclusion

In this paper, we have presented an bilinear immersed finite volume element method for solving the interface problem of the diffusion equation whose domain is formed with multiple materials. This method possesses both the advantages of local conservation in a FVE method and the capability of IFE for handling the jump conditions across material interface. This method can use a Cartesian mesh even if the interface separating the materials is nontrivial, and fast algebraic solvers such as multigrid can be easily applied to generate numerical solutions efficiently for a problem with rather complicated interface. The numerical examples show that this method does have an approximation capability usually expected from bilinear polynomials.

Acknowledgments

This work is partially supported by NSF grant DMS-0713763 and NSERC (Canada). We also appreciate the referee's suggestions and comments which have improved the paper.

References

[1] S. Adjerid and T. Lin. Higher-order immersed discontinuous galerkin methods. Int. J. Info. Syst. Sci., 3(4):555–568, 2007.

[2] S. Adjerid and T. Lin. p-th degree immersed finite element for boundary value problems with discontinuous coefficients, Appl. Numer. Math., to appear.

[3] A. Almgre, J. B. Bell, P. Collela, and T. Marthaler. A cartesian grid method for imcompressible Euler equations in complex geometries. SIAM J. Sci. Comput., 18:1289–1390, 1997.

[4] Y. Arakawa and M. Nakano. An efficient three-dimensional optics code for ion thruster research. In AIAA-3196, 1996.

[5] I. Babuška. The finite element method for elliptic equations with discontinuous coefficients. Computing, 5:207–213, 1970.

[6] I. Babuška, G. Caloz, and J. E. Osborn. Special finite element methods for a class of second order elliptic prolbems with rough coefficients. SIAM J. Numer. Anal., 31:945–981, 1994.

[7] I. Babuška and J. Melenk. The partition of unity method. Int. J. Numer. Methods Eng., 40:727–758, 1997.

[8] I. Babuška and J. E. Osborn. Finite element methods for the solution of problems with rough input data. In P. Grisvard, W. Wendland, and J. R. Whiteman, editors, Singular and Constructive Methods for their Treatment, Lecture Notes in Mathematics, #1121, pages 1–18, New York, 1985. Springer-Verlag.

[9] I. Babuška and J. E. Osborn. Can a finite element method perform arbitrarily badly? Math. Comp., 69(230):443–462, 2000.

[10] J. B. Bell, P. Colella, and H. M. Glaz. A second-order projection method for the incompressible navier-stokes equations. J. Comput. Phys., 85:257–283, 1989.

[11] J. B. Bell and D. L. Marcus. A second-order projection method for variable-density flows. J. Comput. Phys., 101:334–348, 1992.

[12] T. Belytschko, N. Moës, S. Usui, and C. Primi. Arbitrary discontinuities in finite elements. Int. J. Numer. Methods Eng., 50:993–1013, 2001.

[13] M. P. Bendsøe. Optimization of Structural Topology, Shape, and Material. Springer, 1995.

[14] M. P. Bendsøe and N. Kikuchi. Generating optimal topologies in optimal design using a homogenization method. Comp. Meth. Appl. Mech. Engng., 71:197–224, 1988.

[15] M. P. Bendsøe and O. Sigmund. Topology Optimization. Springer, 2nd edition, 2004.

[16] I. Boyd, D. VanGilde, and X. Liu. Monte carlo simulation of neutral xenon flows in electric propulsion devices. J. Propulsion and Power, 14(6):1009–1015, 1998.

[17] J. H. Bramble and J. T. King. A finite element method for interface problems in domains with smooth boundary and interfaces. Adv. Comput. Math., 6:109–138, 1996.

[18] Z. Cai. On the finite volume element method. Numer. Math., 58(7):713–735, 1991.

[19] Z. Cai, J. Mandel, and S. McCormick. The finite volume element method for diffusion equations on general triangulations. SIAM J. Numer. Anal., 28(2):392–402, 1991.

[20] Z. Cai and S. McCormick. On the accuracy of the finite volume element method for diffusion equations on composite grids. SIAM J. Numer. Anal., 27(3):636–655, 1990.

[21] D. Calhoun. A Cartesian grid method for solving the two-dimensional streamfunction-vorticity equations in irregular regions. J. Comput. Phys., 176, 2002.

[22] B. Camp, T. Lin, Y. Lin, and W.-W. Sun. Quadratic immersed finite element spaces and their approximation capabilities. Adv. Comput. Math., 24:81–112, 2006.

[23] P. Chatzipantelidis, V. Ginting, and R. D. Lazarov. A finite volume element method for a non-linear elliptic problem. Numer. Linear Algebra Appl., 12(5-6):515–546, 2005.

[24] P. Chatzipantelidis, R. D. Lazarov, and V. Thomée. Error estimates for a finite volume element method for parabolic equations in convex polygonal domains. Numer. Methods Part. Diff. Eq., 20(5):650–674, 2004.

[25] Z. Chen and J. Zou. Finite element methods and their convergence for elliptic and parabolic interface problems. Numer. Math., 79:175–202, 1998.

[26] C. S. Chew, K. S. Yeo, and C. Shu. A generalized finite-difference (gfd) ale scheme for incompressible flows around moving solid bodies on hybrid meshfreeccartesian grids. J. Comput. Phys., 218:510–548, 2006.

[27] A. J. Chorin. Numerical solution of the Navier-Stokes equations. Math. Comp., 22:745–762, 1968.

[28] D. K. Clarke, M. D. Salas, and H. A. Hassan. Euler calculations for multielement airfoils using cartesian grids. AIAA Journal, 24:353–358, 1986.

[29] A. Dadone and B. Grossman. Progressive optimization of inverse fluid dynamic design problems. Computers & Fluids, 29:1–32, 2000.

[30] A. Dadone and B. Grossman. An immersed body methodology for inviscid flows on cartesian grids. In AIAA, 2002-1059.

[31] D. DeZeeuw and K. G. Powell. An adaptively refined cartesian mesh solver for the Euler equations. J. Comput. Phys., 104:56–68, 1993.

[32] K. Djadel and S. Nicaise. Some refined finite volume element methods for the stokes and navier-stokes systems with corner singularities. J. Numer. Math., 12(4):255–284, 2004.

[33] R. Ewing, Z. Li, T. Lin, and Y. Lin. The immersed finite volume element method for the elliptic interface problems. Math. Comput. Simulat., 50:63–76, 1999.

[34] R. E. Ewing, R. Lazarov, and Y. Lin. Finite volume element approximations of nonlocal reactive flows in porous media. Numer. Methods Part. Diff. Eq., 16(3):285–311, 2000.

[35] A. L. Fogelson and J. P. Keener. Immersed interface methods for neumann and related problems in two and three dimensions. SIAM J. Sci. Comput., 22:1630–1654, 2001.

[36] A. Gersborg-Hansen, M. P. Bendsøe, and O. Sigmund. Topology optimization of heat conduction problems using the finite volume method. Struct. Multidisc. Optim., 31:251–259, 2006.

[37] J. Haslinger and R. A. E. Mäkinen. Introduction to Shape Optimization: Theory, Approximation, and Computation, volume 7 of Advances in Design and Control. SIAM, Philadelphia, 2003.

[38] J. Haslinger and P. Neittaamäki. Finite Element Approximation for Optimal Shape, Material and Topology Design. John Wiley & Sons, Ltd, Chichester, 1996.

[39] X.-M. He, T. Lin, and Y.-P. Lin. Approximation capability of a bilinear immersed finite element space. Numer. Methods Part. Diff. Eq., 24(5):1265–1300, 2008.

[40] B. Heinrich. Finite Difference Methods on Irregular Networks, volume 82 of International Series of Numerical Mathematics. Birkhäuser, Boston, 1987.

[41] G. Hetzer and A. Meir. On an interface problem with a nonlinear jump condition, numerical approximation of solutions. Int. J. Numer. Anal. Model., 4(3-4):519–530, 2007.

[42] D. W. Hewitt. The embedded curved boundary method for orthogonal simulation meshes. J. Comput. Phys., 138:585–616, 1997.

[43] T. Y. Hou and B. T. R. Wetton. Second order convergence of a projection scheme for the incompressible Navier-Stokes equations with boundaries. SIAM J. Numer. Anal., 30:609–629, 1993.

[44] J. Huang and S. Xi. On the finite volume element method for general self-adjoint elliptic problems. SIAM J. Numer. Anal., 35(5):1762–1774, 1998.

[45] D. M. Ingram, D. M. Causon, and C. G. Mingham. Developments in cartesian cut cell methods. Math. Comput. Simulat., 61(3-6):561–572, 2003.

[46] G.-W. Jang, S. Lee, Y. Y. Kim, and D. Sheen. Topology optimization using non-conforming finite elements: three-dismensional case. Int. J. Numer. Methods Eng., 63(6):859–875, 2005.

[47] R. Kafafy, T. Lin, Y. Lin, and J. Wang. 3-d immersed finite element methods for electric field simulation in composite materials. Int. J. Numer. Methods Eng., 64:904–972, 2005.

[48] R. Kafafy, J. Wang, and T.Lin. A hybrid-grid immersed-finite-element particle-in-cell simulation model of ion optics plasma dynamics. Dyn. Cont. Discrete Impulse Syst., 12:1–16, 2005.

[49] D. J. Kirshman and F. Liu. A gridless boundary condition method for the solution of the Euler equations on embedded cartesian meshes with multigrid. J. Comput. Phys., 201:119–147, 2004.

[50] D. V. Le, B. C. Khoo, and J. Peraire. An immersed interface method for viscous incompressible flows involving rigid and flexible boundaries. J. Comput. Phys., 220(6):109–138, 2006.

[51] R. J. LeVeque and Z. Li. The immersed interface method for elliptic equations with discontinuous coefficients and singular sources. SIAM J. Numer. Anal., 34:1019–1044, 1994.

[52] J. Li, Y. Renardy, and M. Renardy. Numerical simulation of breakup of a viscous drop in simple shear flow through a volume-of-fluid method. Phys. Fluids, 12(2):269–282, 2000.

[53] Z. Li. A fast iterative algorithm for elliptic interface problems. SIAM J. Numer. Anal., 35:230–254, 1998.

[54] Z. Li. The immersed interface method using a finite element formulation. Appl. Numer. Math., 27:253–267, 1998.

[55] Z. Li and K. Ito. Maximum principle preserving schemes for interface problems with discontinuous coefficients. SIAM J. Sci. Comput., 23:339–361, 2001.

[56] Z. Li and K. Ito. The Immersed Interface Method: Numerical Solutions of PDEs Involving Interfaces and Irregular Domains, SIAM Frontiers in Applied Mathematics 33. SIAM, Philadelphia, PA, 2006.

[57] Z. Li, T. Lin, Y. Lin, and R.C. Rogers. An immersed finite element space and its approximation capability. Numer. Methods Part. Diff. Eq., 20(3):338–367, 2004.

[58] Z. Li, T. Lin, and X. Wu. New cartesian grid methods for interface problems using finite element formulation. Numer. Math., 96(1):61–98, 2003.

[59] T. Lin, Y. Lin, R.C. Rogers, and L.M. Ryan. A rectangular immersed finite element method for interface problems. In P. Minev and Y. Lin, editors, Advances in Computation: Theory and Practice, Vol. 7, pages 107–114. Nova Science Publishers, Inc., 2001.

[60] T. Lin, Y. Lin, and W.-W. Sun. Error estimation of quadratic immersed finite element methods. Discrete Cont. Dyn. Syst. B, 7(4):807–823, 2007.

[61] T. Lin and J. Wang. An immersed finite element electric field solver for ion optics modeling. In Proceedings of AIAA Joint Propulsion Conference, Indianapolis, IN, July, 2002. AIAA, 2002-4263.

[62] T. Lin and J. Wang. The immersed finite element method for plasma particle simulation. In Proceedings of AIAA Aerospace Sciences Meeting, Reno, NV, Jan., 2003. AIAA, 2003-0842.

[63] I. D. Mishev. Finite volume element methods for non-definite problems. Numer. Math., 83(1):161–175, 1999.

[64] N. Moës, J. Dolbow, and T. Belytschko. A finite element method for crack growth without remeshing. Int. J. Numer. Methods Eng., 46(1):131–150, 1999.

[65] K. Morinishi. A finite difference solution of the Euler equations on non-body fitted grids. Comp. Fluids, 21:331–344, 1992.

[66] Y. Muravlev and A. Shagayda. Numerical modelling of extraction systems in ion thrusters. In IEPC-99-162, 1999.

[67] M. Nakano and Y. Arakawa. Ion thruster lifetime estimation and modeling using computer simulation. In IEPC-99-145, 1999.

[68] Y. Nakayama and P. Wilbur. Numerical simulation of ion beam optics for many-grid systems. In AIAA-2001-3782, 2001.

[69] Y. Okawa and H. Takegahara. Particle simulation on ion beam extraction phenomena in an ion thruster. In IEPC-99-146, 1999.

[70] X. Peng, W. Ruyten, V. Friedly, D. Keefer, and Q. Zhang. Particle simulation of ion optics and grid erosion for two-grid and three-grid systems. Rev. Sci. Instrum., 65(5):1770, 1994.

[71] C. S. Peskin. Flow patterns around heart valves. J. Comput. Phys., 10:252–271, 1972.

[72] C. S. Peskin. Numerical analysis of blood flow in the heart. J. Comput. Phys., 25:220–252, 1977.

[73] A. A. Samarskiĭ and V. B. Andreev. Méthods aux Différences pour Équations Ellipticques. Mir, Moscow, 1978.

[74] O. Sigmund and J. Pertersson. Numerical instabilities in topology optimization: A survey on procedures dealing with checkerboards, mesh-dependencies and local minima. Structural Optimization, 16:68–75, 1998.

[75] R. K. Sinha, R. E. Ewing, and R. D. Lazarov. Some new error estimates of a semidiscrete finite volume element method for a parabolic integro-differential equation with nonsmooth initial data. SIAM J. Numer. Anal., 43(6):2320–2343, 2006.

[76] S. A. Suater and R. Warnke. Composite finite elements for elliptic boudnary value problems with discontinuous coefficients. Computing, 77:29–55, 2006.

[77] N. Sukemar, D.L. Chopp, N. Moës, and T. Belytschko. Modling holes and inclusions by level set in the extended finite-element method. Comput. Methods Appl. Mech. Eng., 190:6183–6200, 2001.

[78] M. Tartz. Validation of a grid-erosion simulation by short-time erosion measurements. In IEPC 99-147, 1999.

[79] H. Wang. An improved wpe method for solving discontinuous fokker-planck equations. Int. J. Numer. Anal. Model., 5(1):1–23, 2008.

[80] A. Wiegmann and K. Bube. The immersed interface method for nonlinear differential equations with discontinuous coefficients and singular sources. SIAM J. Numer. Anal., 35:177–200, 1998.

[81] A. Wiegmann and K. Bube. The explicit-jump immersed interface method: Finite difference methods for pdes with piecewise smooth solutions. SIAM J. Numer. Anal., 37:827–862, 2000.

[82] H. Wu and R. Li. Error estimates for finite volume element methods for general second-order elliptic problems. Numer. Methods Part. Diff. Eq., 19(6):693–708, 2003.

[83] Y. Gong, B. Li, and Z. Li. Immersed-interface finite-element methods for elliptic interface problemswith non-homogeneous jump conditions. SIAM J. Numer. Anal., 46:472-495, 2008.

[84] Y. C. Zhou and G. W. Wei. On the fictitious-domain and interpolation formulations of the matched interface and boundary (MIB) method. J. Comput. Phys., 219(1):228–246, 2006.

[85] Y. C. Zhou, S. Zhao, M. Feig, and G. W. Wei. High order matched interface and boundary method for elliptic equations with discontinuous coefficients and singular sources. J. Comput. Phys., 213(1):1–30, 2006.

[86] S.-H. Zhu, G.-W. Yang, and W.-W. Sun. Convergence and stability of explicit/implicit schemes for parabolic equations with discontinuous coefficients Int. J. Numer. Anal. Model., 1(2):131–146, 2004.